Hindawi
Journal of Chemistry
Volume 2020, Article ID 2928189, 10 pages
https://doi.org/10.1155/2020/2928189

Research Article

Preparation and Photocatalytic Properties of N-Doped Graphene/TiO_2 Composites

Jing Liu[1], **Kun-Yu Chen**[1], **Jie Wang**[2], **Min Du**[3], **Zheng-Yang Gao**[1], **and Chun-Xiao Song**[1]

[1]*School of Municipal and Environmental Engineering, Shandong Jianzhu University, Jinan 250101, China*
[2]*Shandong Huankeyuan Environmental Engineering Co. Ltd., Jinan 250013, China*
[3]*Shandong Engineering Consulting Institute, Jinan 250014, China*

Correspondence should be addressed to Jing Liu; liujing19691109@sdjzu.edu.cn

Received 7 June 2019; Revised 10 February 2020; Accepted 19 February 2020; Published 16 March 2020

Academic Editor: Muhammad J. Habib

N-doped graphene (NG)/TiO_2 composites were prepared by a two-step hydrothermal method using HF as the surface etchant and urea as the nitrogen source. The morphology, structure, and bonding conditions of the NG/TiO_2 composites were characterized by X-ray diffraction (XRD), field emission scanning electron microscopy (FESEM), X-ray photoelectron spectroscopy (XPS), Raman spectroscopy, UV-visible diffuse reflectance spectroscopy (UV-Vis DRS), and photoluminescence (PL) spectroscopy. The effects of NG on the lifetime of photogenerated electron-hole pairs, adsorption capacity, and photocatalytic activity of the composite photocatalysts were also investigated. The photocatalytic activity was evaluated under ultraviolet light and sunlight irradiation. The recovery testing was completed under ultraviolet light irradiation. The results show that TiO_2 was uniformly loaded on the NG surface by chemical bonding. The introduction of NG effectively inhibited the recombination of photogenerated electron-hole pairs and improved both the adsorption capacity and photocatalytic activity of the composites. The 7 wt % NG/TiO_2 showed the best adsorption capacity of methyl orange (MO). The best photocatalytic activity occurred for 5 wt % NG/TiO_2 composites, and after four recovery tests, the photocatalytic degradation of MO under 60 min ultraviolet light irradiation exceeded 90%.

1. Introduction

In recent years, TiO_2 has become widely used in the field of photocatalysis because of its strong oxidizing ability, high chemical stability, low cost, nontoxicity, and environmental friendliness [1, 2]. TiO_2 can undergo photocatalytic reactions under mild reaction conditions and will generate hydroxyl radicals (·OH) [3, 4]. However, TiO_2 only responds to ultraviolet (UV) light, which is less than 5% of the solar spectrum, leading to a very inefficient use of solar energy. Also, the recombination rate of photoexcited charge carriers is high, so the quantum efficiency of TiO_2 is low. Therefore, effectively suppressing the recombination of photoexcited carriers in the photocatalytic processes and improving the utilization of solar light are urgent problems to be solved.

Graphene is a two-dimensional carbon material formed by a single layer of C atoms with sp^2 hybridization. It has high conductivity, high stability, and a large specific surface area (theoretical value of 2630 m^2/g). Since nitrogen atoms have an atomic radius similar to that of carbon atoms, the carbon structure can be doped with nitrogen atoms serving as electron donors, and the resulting N-doped graphene (NG) exhibits many new properties including a band gap, n-type conductivity, and increased free carrier density, thereby improving the conductivity and stability of graphene [5–7]. NG can provide a carrier for TiO_2 photogenerated electrons, reduce the recombination of photoexcited carriers, and improve the efficiency of photocatalytic reactions. Therefore, NG/TiO_2 composites may be ideal new photocatalysts.

Compared with the methods of precipitation and sol-gel, the material prepared by the hydrothermal method has the advantages of high purity, adjustable particle size, adjustable morphology and crystal surface, and simple reaction conditions. Yan et al. [8] prepared RGO/TiO_2 composites with high photocatalytic performance by a two-step hydrothermal method. Based on this previous work, the raw materials

were modified and new NG/TiO_2 composites were also synthesized by a two-step hydrothermal method. In this work, $Ti(SO_4)_2$ was used as the titanium source, urea as the nitrogen source, and HF as the surface etchant. The samples were characterized by various methods to determine the morphology and structure of NG/TiO_2. The effects of introducing NG on photogenerated electron-hole pair lifetimes, adsorption performance, and photocatalytic performance were also studied. The photocatalytic properties of the composites for the degradation of methyl orange (MO) were tested under UV and sunlight conditions, and the catalysts were tested several times to investigate their cyclability.

2. Experimental

2.1. Materials. Titanium sulfate (Ti $(SO_4)_2$, ≥97.0%), hydrofluoric acid (HF, ≥ 40.0%), absolute ethanol (≥99.7%), urea (≥99.5%), graphite powder (≥99.9%), potassium permanganate ($KMnO_4$, ≥99.5%), sodium nitrate ($NaNO_3$, ≥99.0%), sulfuric acid (H_2SO_4, 95.0~98.0%), hydrogen peroxide (H_2O_2, ≥40%), and methyl orange were all purchased from Sinopharm Chemical Reagent Co., Ltd. (Shanghai, China).

2.2. Synthesis of NG/TiO_2 Composites

2.2.1. Preparation of Nano-TiO_2. The preparation of anatase nano-TiO_2 was completed using the hydrothermal method. 30 mL HF (160 mmol/L), 50 mL H_2O, and 192 mg $Ti(SO_4)_2$ were added to a plastic beaker. Because $Ti(SO_4)_2$ can be hydrolyzed, the HF was added to water first, and then the $Ti(SO_4)_2$ was added to the mixture. Next, the prepared solution was sonicated and then magnetically stirred for 15 min each, followed by the transfer of the reaction solution to a 100 mL Teflon-lined reactor, and subsequently incubated at 180°C for 12 hours. Finally, the obtained product was centrifuged, and the impurities were removed by washing with absolute ethanol and deionized water several times, and the sample was dried in a vacuum oven at 60°C for 12 hours. The obtained white powder was anatase-type nano-TiO_2 powder.

2.2.2. Preparation of NG. A modified Hummers method was used for graphene oxide (GO) preparation. First, 30 mL of the GO dispersion was added to a beaker, and then urea was added in a mass ratio of 1 : 5 GO to urea. After magnetically stirring for 30 minutes, the solution was transferred to a Teflon-lined reactor, incubated at 160°C for 3 hours, naturally cooled, and then centrifuged several times, giving the final product NG, after lyophilization.

2.2.3. Preparation of NG/TiO_2 Composites. 60 mg of TiO_2 powder, different masses of NG (1%, 3%, 5%, 7%, 9% by mass of TiO_2), and 50 mL of water were added to test tubes. After sonication for three hours, each mixed solution was poured into a 100 mL Teflon-lined reactor and was incubated at 180°C for 12 hours. The obtained product was centrifuged, and the impurities were removed by washing with absolute ethanol and deionized water several times, and the sample was dried in a vacuum oven at 60°C for 12 hours. The obtained powders were NG/TiO_2 composites.

2.3. Characterization. X-ray diffraction (XRD, Bruker AXS D8 Advance) with a Cu target and Kα radiation ($\lambda = 0.15406$ nm) was used for phase identification of the samples in the range of 10°–80°. The morphology of the samples was examined by a field emission scanning electron microscope (FESEM, Hitachi SU8010). The chemical state of the sample was analyzed by X-ray photoelectron spectroscopy (XPS, Escalab 250 XI), and the structure of the sample was analyzed using Raman spectroscopy (RAMAN, Renishaw RM 2000). The absorption range and absorption properties of the sample were measured by ultraviolet-visible diffuse reflectance spectroscopy (UV-VIS DRS, PerkinElmer Lambda 650) and the recombination efficiency of the sample electron-hole pairs was characterized using photoluminescence spectroscopy (PL, HR 320).

2.4. Photocatalytic Activity

2.4.1. Suction and Desorption Balance Tests. 0.1 g of each composite with different NG concentrations was placed in 100 mL of a solution with 20 mg/L MO (pH = 3). This mixture was stirred in the dark and samples were taken every 10 minutes. After centrifugation, the supernatant was taken, and the absorbance was measured at $\lambda_{max} = 464$ nm using an UV-visible spectrophotometer to calculate the residual dye concentration. The MO adsorption amount of the composites was calculated according to [9]

$$q = \frac{(Ca0 - Cat)V}{m}, \quad (1)$$

where q is the adsorption capacity; $Ca0$ is the initial concentration of MO; Cat is the concentration of MO when adsorbed; V is the solution volume; and m is the mass of the adsorbent.

2.4.2. Photocatalytic Degradation Test. 0.1 g of each composite having a different NG doping ratio was added to 100 mL of a 20 mg/L MO solution (pH = 3), and the mixture was stirred for one hour in the dark. In order to study the photocatalytic degradation ability of composites, catalytic reactions were carried out under ultraviolet light and sunlight, respectively. In order to study the effect of H_2O_2 on the reaction rate of the composites, 2 mL H_2O_2 was added to samples under ultraviolet light and sunlight, respectively. The ultraviolet light source was a 250 W high-pressure mercury lamp (365 nm ultraviolet light), which was 15 cm away from the mixture and was sampled every 10 min. After centrifugation, the supernatant was taken, and the absorbance was measured by a UV-visible spectrophotometer to calculate the photocatalytic efficiency. The solar photocatalytic test was conducted over a 5-hour period outdoors on a sunny day. The photocatalytic efficiency was calculated according to [9]

$$\eta = \frac{C\,d0 - C\,dt}{C\,d0} \times 100\%, \quad (2)$$

where *Cd0* is the initial concentration of MO and *Cdt* is the concentration of MO when the reaction time is *t*.

2.4.3. Recovery Test. 0.1 g of 5 wt % NG/TiO_2 was added to 100 mL of a 20 mg/L MO solution (pH = 3) and stirred for 60 min in the dark to bring the MO into an adsorption equilibrium. The photocatalytic reaction was then carried out under a UV lamp and sampled at 60 min. After centrifugation, the supernatant was taken, and the absorbance was measured by a UV-visible spectrophotometer to calculate the photocatalytic efficiency, and the calculation formula was the same as formula (2). Then, the precipitate and the photocatalyst were washed together and dried, and photocatalytic testing was repeated after the recovery.

3. Results and Discussion

3.1. XRD. Considering the XRD spectrum of TiO_2 and NG/TiO_2 composites (Figure 1), the 2θ values of 25.51°, 38.02°, 48.15°, 54.04°, 55.20°, 62.87°, 68.95°, 70.36°, and 75.21° correspond to the crystal surface characteristic diffraction peaks of (101), (004), (200), (105), (211), (204), (116), (220), and (215) of anatase phase TiO_2 (JCPDS 21-1272), respectively. These indicate that the prepared TiO_2 and NG/TiO_2 composites are mainly anatase crystal types. The diffraction peaks of the NG/TiO_2 composites are significantly weaker than those of TiO_2, which is due to the interaction between NG and TiO_2. In the NG/TiO_2 composites, the (002) characteristic diffraction peak of graphene did not appear near $2\theta = 26°$ because this diffraction peak overlaps with the (101) crystal plane diffraction peak of the anatase phase TiO_2 [10, 11].

When calculated by the Scherrer equation, the TiO_2 nanoparticles were 43 nm. The Scherrer equation is as follows:

$$D = \frac{K\gamma}{B\cos\theta}. \quad (3)$$

D is the average thickness of the crystal grains perpendicular to the crystal plane direction, nm; K is the Scherrer constant, 0.89; γ is the X-ray wavelength, which is 0.154056 nm; B is the half-height width of the diffraction peak of the measured sample; θ is the Bragg diffraction angle.

3.2. FESEM. From Figure 2, it can be seen that TiO_2 and NG/TiO_2 composites have undergone agglomeration phenomena, because there are a few crystal surfaces on the surface of photocatalyst, due to HF etching. The etching mainly occurs on the high surface energy crystal face (001) and continues along the (001) direction [8], making it easy for particles to agglomerate in order to achieve a stable state. Figure 2(b) is the SEM image of the NG/TiO_2 composites. The morphology of TiO_2 did not change and the loading was good through the secondary hydrothermal treatment. Some of the N-doped graphene thin layers are stacked together to form a multilayer structure. This edge curl and fold appearance was attributed to the defect structure caused by the nitrogen-doped graphene crystal [12].

3.3. XPS. The chemical composition of NG/TiO_2 nanocomposites was investigated by XPS. The characteristic peaks of C, F, N, O, and Ti can be observed in Figure 3(a). C 1*s* (Figure 3(b)) has a binding energy of 284.3 eV, indicating the presence of a C-C bond, which is a characteristic peak for graphene. The peaks at binding energies of 285.5 and 288.8 eV correspond to C-O and C=O, respectively, and were caused by possible residual hydroxyl functional groups of graphene [13]. Figure 3(c) is the deconvoluted peak of O 1*s*, where the peak at 531.3 eV corresponds to Ti-O-C, the peak at 530.6 eV corresponds to C=O and O=C-OH, and the peak at 533.4 eV corresponds to C-O [14]. In Figure 3(d), the characteristic peaks of Ti 2*p*3/2 and Ti 2*p*1/2 appeared at binding energies of 458.7 and 464.5 eV, respectively, which confirmed the existence of TiO_2 [15]. The peak at 459.2 eV corresponds to C-Ti, indicating that there is an interaction between TiO_2 and NG. The N 1*s* (Figure 3(e)) peak has binding energy at 399.5 eV, indicating that there may be C-N present, proving that the N atom has been doped into the structure of graphene. The F 1*s* (Figure 3(f)) spectra can be deconvoluted into two peaks. The peak located at a binding energy of 684.7 eV was caused by the exchange of ligands between F and hydroxyl groups on the surface of TiO_2 to form ≡Ti-F, and F^- chemisorbed on the surface of the nano-TiO_2 [16]. The peak near 690.2 eV indicated that F is doped into the TiO_2 lattice [17].

3.4. Raman Spectrum. It can be seen from the Raman spectrum (Figure 4(a)) that characteristic Raman scattering peaks of anatase phase TiO_2 were observed at 144.4 cm^{-1} (E_g), 395.9 cm^{-1} (B_{1g}), 515.4 cm^{-1} (A_{1g}) and 636.3 cm^{-1} (E_g). Figure 4(b) shows that the characteristic Raman scattering peaks for the D-band and G-band of graphene were observed near 1364 cm^{-1} and 1578 cm^{-1}, respectively. After the formation of the NG/TiO_2 composites, the characteristic Raman peaks of the anatase TiO_2 still existed, and the Raman peaks of the composites moved toward higher wavenumbers, indicating that a chemical interaction between NG and TiO_2 molecules took place [18, 19]. However, due to the addition of NG, the impurity level or defect level will appear in the spectra of the composites, and the appearance of the impurity level or defect level will also cause the Raman peaks to move toward higher wavenumbers [18–20].

3.5. UV-VIS DRS. The UV-visible diffuse reflectance spectrum (Figure 5(a)) shows that pure TiO_2 has a light absorption range below 400 nm and can only absorb ultraviolet light. This is due to the electron transfer from the valence band (O 2*p*) to the conduction band (Ti 3*d*). Compared with pure TiO_2, the light absorption boundary of the NG/TiO_2 composites was red-shifted, and the absorption range of the photocatalyst was extended to the visible light region. The absorption intensity was also improved due to the introduction of nitrogen atoms into the carbon grid of graphene. TiO_2 grew on the N-doped graphene layer in situ through Ti-O-C bonding and hybridized with the C 2*p* and O 2*p* atomic orbitals under high

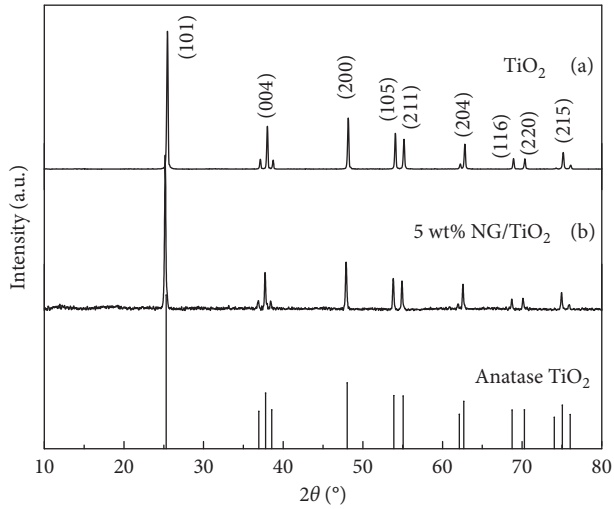

Figure 1: XRD patterns of TiO_2 and NG/TiO_2.

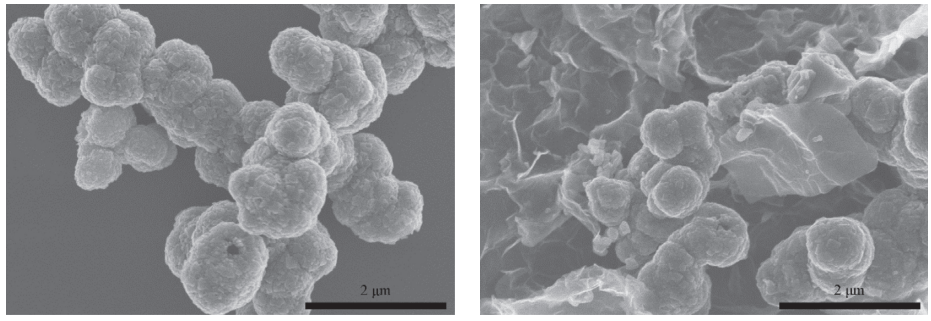

Figure 2: FESEM images of TiO_2 (a) and NG/TiO_2 (b).

temperature and pressure [21]. This resulted in the increase of the valence band edge, thereby reducing the width of the forbidden band [22], and showed strong light absorption with visible light response ability. The band gap energies of TiO_2, 3 wt % NG/TiO_2, 5 wt % NG/TiO_2, and 7 wt % NG/TiO_2 were calculated by formula $E_g = 1240/\lambda$ and were approximately 3.18 eV, 2.98 eV, 2.92 eV, and 2.96 eV, respectively (Figure 5(b)).

3.6. Photoluminescence. The photoluminescence spectrum is a way to characterize the electron-hole pair recombination efficiency: low emission intensity indicates that the recombination rate of photogenerated electron-hole pairs is slow, and the separation of electrons and holes is effective [23], which is beneficial to photocatalytic reaction. The spectrum in Figure 6 shows that the photoluminescence of the NG/TiO_2 composites with different amounts introduced, including 0 wt %, 1 wt %, 3 wt %, 5 wt %, 7 wt %, and 9 wt %. The emission intensity of pure titanium dioxide is the highest, indicating that the electron-hole pair has the fastest recombination rate and the lowest photocatalytic efficiency. The presence of NG can be used as a carrier of photogenerated electrons, which has charge transfer with the semiconductor and can effectively inhibit the recombination of photogenerated electron-hole pairs. 5 wt % NG/TiO_2 has the lowest emission intensity, indicating that the introduction of 5 wt % NG can transfer electrons well and can effectively separate electrons and holes, and therefore the photocatalytic effect will be the most significant. Introducing insufficient amounts of NG is the reason that NG, as a carrier, cannot transport the photogenerated electrons completely and effectively, and some of the excess photogenerated electrons will recombine with holes, affecting the photocatalytic reaction efficiency. Excessive NG can reduce the effective components of photoelectron-hole pairs, and at the same time, the photoelectron hole can use NG as the recombination center to recombine within it [24], affecting the photocatalytic reaction efficiency.

In general, different characterization techniques verify and compensate for each other and comprehensively evaluate the composites from different angles.

3.7. Photocatalytic Activity

3.7.1. Suction and Desorption Balance Tests. The adsorption of dye by a photocatalyst plays an important role in dye degradation [25, 26]. MO is a monosulfonate azo compound. Under acidic conditions, the $-SO^{3-}$ in MO interacted with the positively charged center on the surface of TiO_2 and adsorbed on the surface in a vertical manner. Such an adsorption mode left a small amount of MO on the surface of

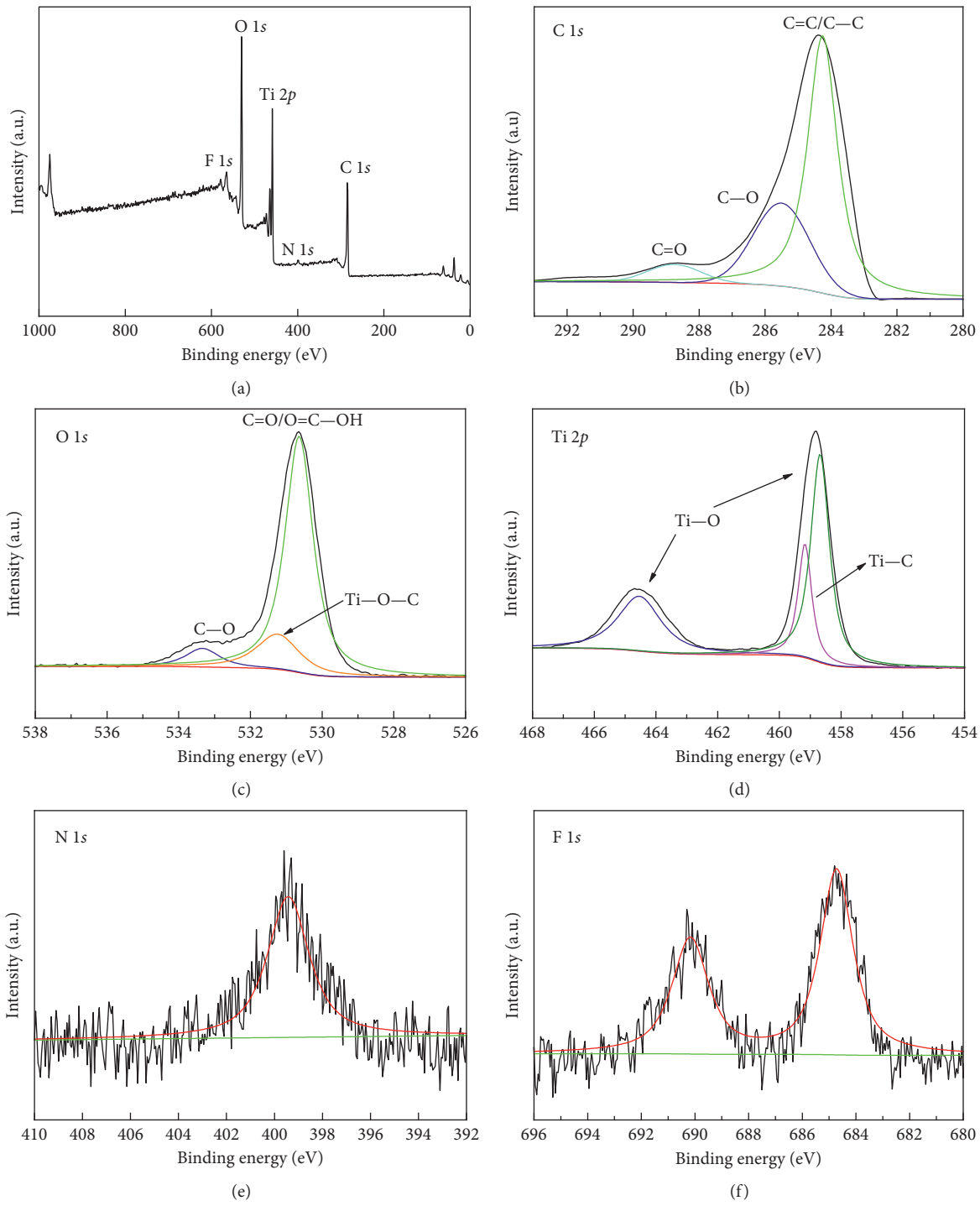

Figure 3: (a) Full XPS spectrum of NG/TiO_2, XPS spectra of C 1s (b), O 1s (c), Ti 2p (d), N 1s (e), and F 1s (f) in NG/TiO_2.

TiO_2 [27]. Figure 7 shows the adsorption curves of MO for samples with different NG doping. The amount of adsorption of MO on the sample increased with time, and the adsorption was effectively saturated after 60 min. The adsorption performance of the composites with different NG loadings was better than that of TiO_2, and the adsorption amount increased at first and then decreased with the increase of NG loading. 7 wt % NG/TiO_2 had the best adsorption performance, and the adsorption capacity after 60 min was 9.27 mg/g. This amount of NG effectively improved the adsorption performance of TiO_2, but the amount of NG had a limit. This was because NG itself had a very large specific surface area and provided more sites for the adsorption of MO. However, as the amount of NG became too large, it reduced the specific surface area due to overlapping with itself, which then affected the adsorption of MO by the catalyst.

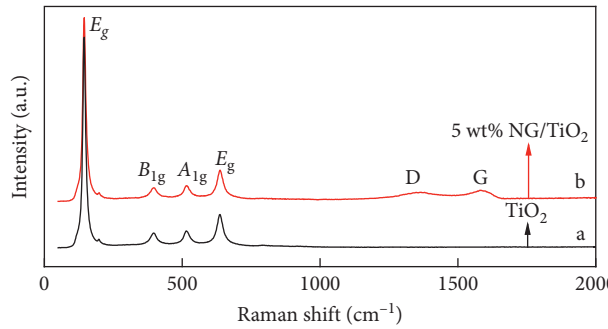

Figure 4: Raman spectra of TiO_2 (a) and 5 wt % NG/TiO_2 (b).

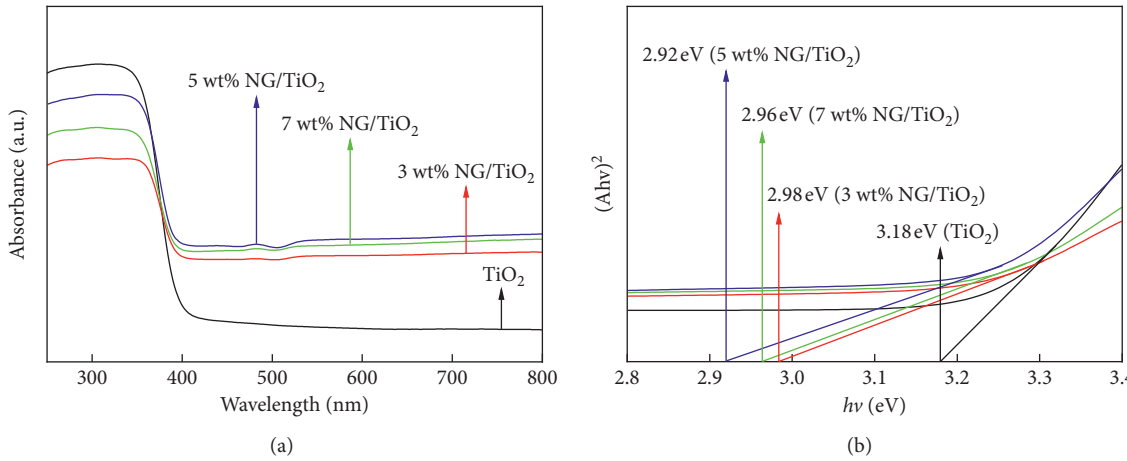

Figure 5: UV-visible diffuse reflectance spectra of TiO_2 and NG/TiO_2 (a); optical band gap determination of TiO_2 and NG/TiO_2 (b).

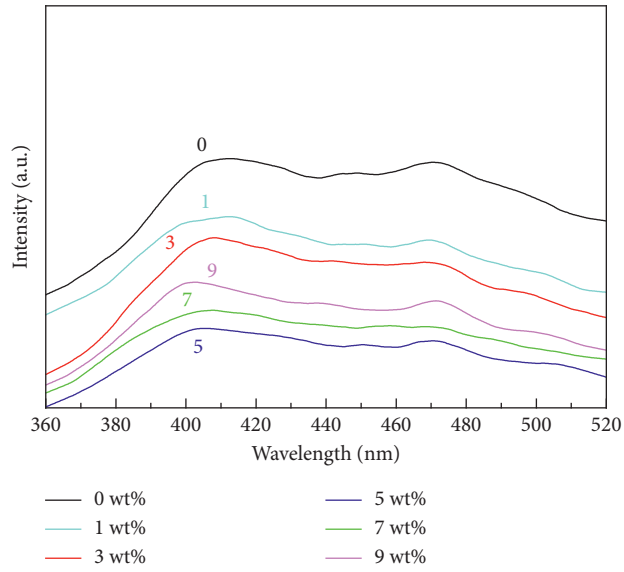

Figure 6: Photoluminescence spectra of NG/TiO_2 composites with different contents of NG.

3.7.2. Photocatalytic Degradation Test. From Figure 8(a) and Table 1, it can be seen that 5 wt % NG/TiO_2 has the highest photocatalytic efficiency under UV(H_2O_2) condition. The degradation efficiency of 5 wt % NG/TiO_2 for MO reached 68.43% in 10 min and 100% in 30 min under UV(H_2O_2) condition. The degradation efficiency of TiO_2 for MO reached 65.14% in 30 min under UV(H_2O_2) condition. The degradation efficiencies of other NG-added photocatalysts for MO

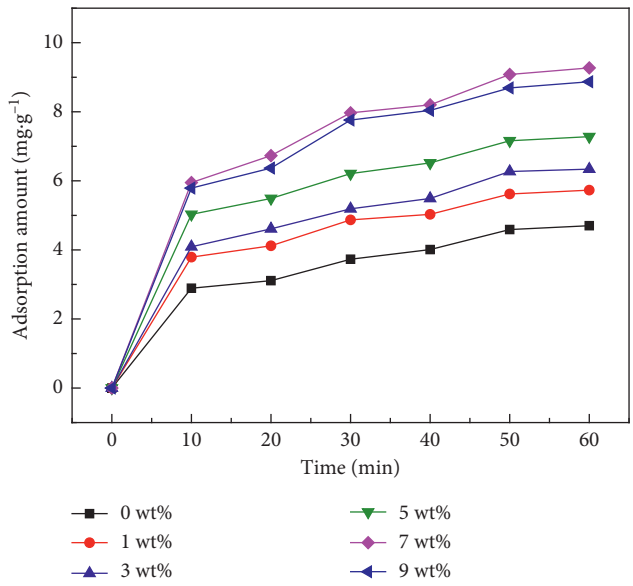

Figure 7: Adsorption activity of NG/TiO_2 composites with different concentrations of NG.

reached 97.53% (7 wt % NG/TiO_2), 92.31% (9 wt % NG/TiO_2), 91.53% (3 wt % NG/TiO_2), and 82.41% (1 wt % NG/TiO_2) in 30 min under UV(H_2O_2) condition. From Figure 8(b) and Table 1, it can be seen that the degradation efficiency of 5 wt % NG/TiO_2 for MO reached 82.91% in 30 min and 100% in 60 min under UV condition. The degradation efficiency of TiO_2 for MO reached 43.02% in 30 min under UV condition. The degradation efficiencies of other NG-added photocatalysts for MO reached 72.54% (7 wt % NG/TiO_2), 68.28% (9 wt % NG/TiO_2), 64.03% (3 wt % NG/TiO_2), and 57.83% (1 wt % NG/TiO_2) in 30 min under UV condition. From Figure 8(c) and Table 2, it can be seen that the degradation efficiency of 5 wt % NG/TiO_2 for MO reached 98.9% in 120 min under sunlight (H_2O_2) condition. The degradation efficiency of TiO2 for MO reached 59.24% in 120 min under sunlight (H_2O_2) condition. The degradation efficiencies of other NG-added photocatalysts for MO reached 89.46% (7 wt % NG/TiO_2), 81.08% (9 wt % NG/TiO_2), 77.91% (3 wt % NG/TiO_2), and 70.26% (1 wt % NG/TiO_2) in 120 min under sunlight (H_2O_2) condition. From Figure 8(d) and Table 2, it can be seen that the degradation efficiency of 5 wt % NG/TiO_2 for MO reached 46.97% in 120 min under sunlight condition. The degradation efficiency of TiO2 for MO reached 26.29% in 120 min under sunlight condition. The degradation efficiencies of other NG-added photocatalysts for MO reached 42.97% (7 wt % NG/TiO_2), 39.08% (9 wt % NG/TiO_2), 35.76% (3 wt % NG/TiO_2), and 33.27% (1 wt % NG/TiO_2) in 120 min under sunlight condition. The experimental results showed that the degradation rate under sunlight conditions was lower than that under ultraviolet light. This was because UV was a single wavelength high-pressure mercury lamp at 365 nm, whereas the sunlight was a full-spectrum light source containing ultraviolet and visible light in each wavelength band. Whether it was pure TiO_2 or the NG/TiO_2 composites, the degradation efficiency under UV conditions was higher than sunlight, and the addition of H_2O_2 in the photocatalytic system promoted the photocatalytic degradation performance of the photocatalyst [28]. Compared with pure TiO_2, the photocatalytic efficiency of the composites increased with the addition of NG. As the NG content increased, the catalytic performance of different photocatalysts increased at first and then decreased. Comparing NG/TiO_2 with two other photocatalysts (RGO/TiO_2 [9] and N-TiO_2/RGO [29]) under the same conditions, the results showed that NG/TiO_2 exhibited the highest degradation efficiency for MO. The main reasons are as follows: (1) NG had a large specific surface area and an extremely high electron mobility. The combination of NG and TiO_2 significantly increased the specific surface area and electron mobility of the catalyst. As the photon contact probability increased, the absorption intensity of the dye molecules and photons increased. The higher electron mobility increased the photogenerated electron transfer rate of TiO_2, inhibited the photogenerated electron-hole pair recombination, and thus had better photocatalytic performance. (2) N-doping narrowed the forbidden bandwidth of the photocatalyst, improved the responsivity of the photocatalyst in the visible light region, and thereby improved the utilization of sunlight. (3) With the increase of NG content, the effective component (TiO_2) of the photocatalyst decreased, and the photocatalytic efficiency also decreased. The reason why the 7 wt % NG/TiO_2 with the largest adsorption capacity did not exhibit the best photocatalytic performance may be due to the decrease of TiO_2 in the photocatalyst, which led to the photocatalyst not being able to completely oxidize the MO adsorbed on the surface.

3.7.3. Recovery Test. In order to evaluate the chemical stability of the catalyst and the prospective industrial applications, a 5 wt % NG/TiO_2 sample with excellent photocatalytic performance was subjected to multiple recovery cycle tests under ultraviolet conditions. Figure 9 shows the degradation

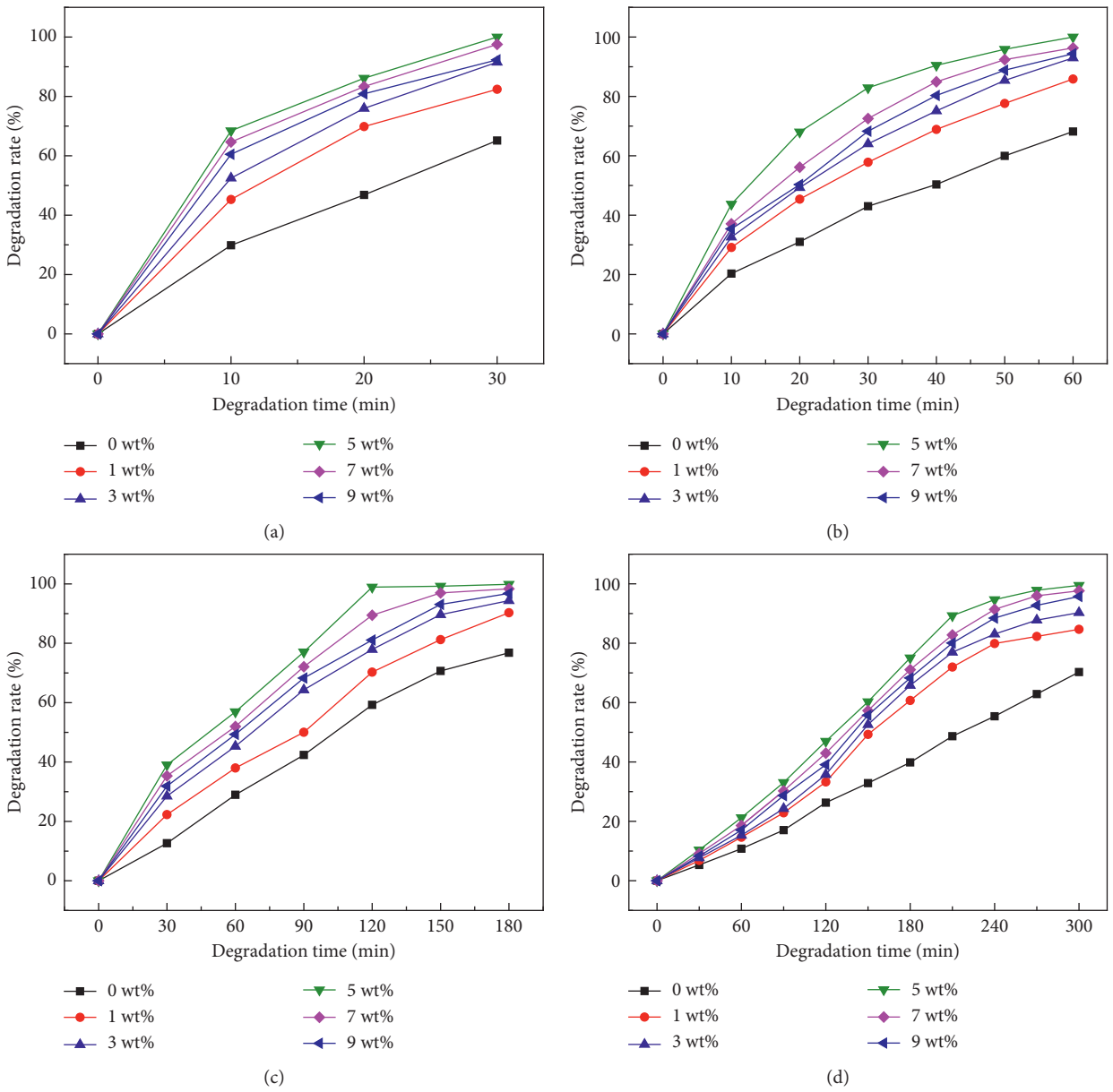

Figure 8: (a) Degradation efficiency of UV photocatalytic degradation of MO in different samples under H_2O_2 conditions with reaction time; (b) the degradation efficiency of UV by photocatalytic degradation of MO in different samples with the reaction time curve; (c) the degradation efficiency of solar photocatalytic degradation of MO in different samples under H_2O_2 conditions with reaction time curve; (d) degradation efficiency of photocatalytic degradation of MO by different samples with reaction time.

Table 1: Photocatalytic degradation efficiency of MO in different samples under UV and UV (H_2O_2) conditions.

UV(H_2O_2) UV (min)	TiO_2 (%)	1 wt % (%)	3 wt % (%)	5 wt % (%)	7 wt % (%)	9 wt % (%)
10	29.86	45.29	52.48	68.43	64.66	60.51
	20.32	29.13	32.61	43.71	37.08	35.37
20	46.83	69.85	75.97	86.13	83.31	80.87
	31.01	45.39	49.29	68.03	56.15	50.31
30	65.14	82.41	91.53	100.00	97.53	92.31
	43.02	57.83	64.03	82.91	72.54	68.28

rate of MO in the sample for each 60 min cycle in tests of one to five cycles. The degradation rate of the photocatalyst was reduced in recycling. On one hand, the MO adsorbed during the cycle was not completely degraded, blocking the exchange channel of the substance and affecting the degradation efficiency of the catalyst. On the other hand, a small amount of

Table 2: Photocatalytic degradation efficiency of MO in different samples under sunlight and sunlight (H_2O_2) conditions.

Sunlight (H_2O_2) and sunlight (min)	TiO_2 (%)	1 wt % (%)	3 wt % (%)	5 wt % (%)	7 wt % (%)	9 wt % (%)
30	12.64	22.29	28.53	39.03	35.32	31.89
	5.32	6.80	7.71	10.36	9.13	8.29
60	28.97	37.98	45.31	56.94	51.97	49.32
	10.79	14.65	15.29	21.24	18.59	17.09
90	42.37	50.01	64.32	77.07	72.09	68.29
	17.03	22.87	24.29	33.09	30.26	28.67
120	59.24	70.26	77.91	98.90	89.46	81.08
	26.29	33.27	35.76	46.97	42.97	39.08

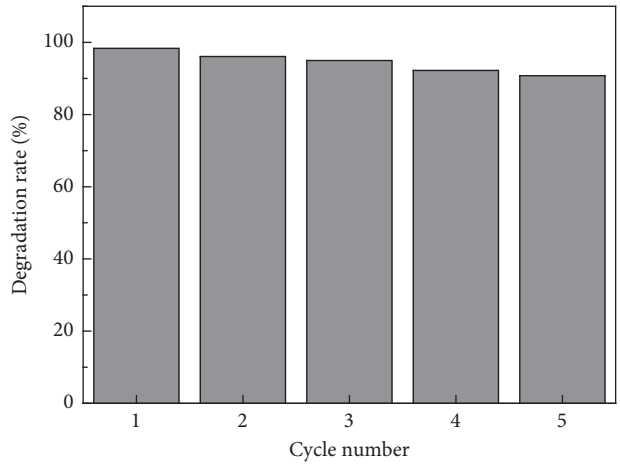

Figure 9: Recovery test of 5 wt % NG/TiO_2.

sample was lost in the recycling process. The photocatalyst degradation rate was 90.77% in the 5th cycle, showing it was stable and ideal for industrial applications.

4. Conclusions

NG/TiO_2 composites were successfully synthesized by a two-step hydrothermal method with HF as the surface etchant and urea as the nitrogen source of NG. The morphology was optimal, and the chemical bond between NG and TiO_2 resulted in a firm loading. By adding different amounts of NG, the recombination of photogenerated electron-hole pairs was effectively suppressed, the lifetime of carriers was prolonged, and the ability to respond to visible light was improved. The photocatalytic performance test showed that NG/TiO_2 composites had better adsorption performance and photocatalytic performance than pure TiO_2. Specifically, 7 wt % NG/TiO_2 showed the best adsorption effect on methyl orange, and the adsorption capacity after 60 min of reaction time was 9.27 mg/g. However, 5 wt % NG/TiO_2 showed the best photocatalytic activity. Under the conditions of UV light with the addition of 2 mL H_2O_2, the degradation efficiency of methyl orange reached 100% after 30 min, and it was completely degraded after 60 min. Under the conditions of sunlight and 2 mL of H_2O_2, the degradation efficiency of methyl orange reached 98.9% after 120 min, and the degradation efficiency reached 99.85% after 180 min. The degradation efficiency of methyl orange reached 94.67% after 240 min in pure solar illumination. After 300 min of degradation time, the efficiency reached 99.48%. After five reaction cycles, the degradation rate of methyl orange was still more than 90% at 60 min, showing a stable photocatalytic activity. Therefore, NG/TiO_2 composites are a new type of photocatalytic material that is ideal for industrial applications.

Data Availability

The data used to support the findings of this study are available from the corresponding author upon request.

Conflicts of Interest

The authors declare that they have no conflicts of interest.

Acknowledgments

The authors acknowledge the support of Junan County, Shandong Province, Industry-University-Research Fund Project.

References

[1] B. O'Regan and M. Grätzel, "A low-cost, high-efficiency solar cell based on dye-sensitized colloidal TiO_2 films," *Nature*, vol. 353, no. 6346, pp. 737–740, 1991.

[2] M. Elfatih, C. Jing, G. Liu, D. Zhu, and J. Cai, "Enhanced photocatalytic degradation of methyl orange dye under the

daylight irradiation over CN-TiO_2 modified with OMS-2," *Materials*, vol. 7, no. 12, pp. 8024–8036, 2014.

[3] M. A. Aramendía, A. Marinas, J. M. Marinas, J. M. Moreno, and F. J. Urbano, "Photocatalytic degradation of herbicide fluroxypyr in aqueous suspension of TiO_2," *Catalysis Today*, vol. 101, no. 3-4, pp. 187–193, 2005.

[4] D. Chatterjee and S. Dasgupta, "Visible light induced photocatalytic degradation of organic pollutants," *Journal of Photochemistry and Photobiology C: Photochemistry Reviews*, vol. 6, no. 2-3, pp. 186–205, 2005.

[5] S.-M. Li, S.-Y. Yang, Y.-S. Wang et al., "N-doped structures and surface functional groups of reduced graphene oxide and their effect on the electrochemical performance of supercapacitor with organic electrolyte," *Journal of Power Sources*, vol. 278, no. 4, pp. 218–229, 2015.

[6] G. Tian, L. Liu, Q. Meng, and B. Cao, "Facile synthesis of laminated graphene for advanced supercapacitor electrode material via simultaneous reduction and N-doping," *Journal of Power Sources*, vol. 274, pp. 851–861, 2015.

[7] D. Wang, Y. Min, Y. Yu, and B. Peng, "A general approach for fabrication of nitrogen-doped graphene sheets and its application in supercapacitors," *Journal of Colloid and Interface Science*, vol. 417, no. 3, pp. 270–277, 2014.

[8] W. Y. Yan, Q. Zhou, X. Chen et al., "Preparation of reduced graphene oxide/nano TiO_2 composites by two-step hydrothermal method and their photocatalytic properties," *Acta Materiae Compositae Sinica*, vol. 33, no. 1, pp. 123–131, 2016.

[9] C. X. Li, H. Z. Jin, Z. Z. Yang et al., "Preparation and photocatalytic properties of mesoporous RGO/TiO_2 composites," *Journal of Inorganic Materials*, vol. 32, no. 4, pp. 357–364, 2017.

[10] L. Zhang, J. Zhang, H. Jiu, C. Ni, X. Zhang, and M. Xu, "Graphene-based hollow TiO_2 composites with enhanced photocatalytic activity for removal of pollutants," *Journal of Physics and Chemistry of Solids*, vol. 86, pp. 82–89, 2015.

[11] Q. I. Qi, Y. Q. Wang, S. S. Wang et al., "Preparation of reduced graphene oxide/TiO_2 nanocomposites and their photocataiytic properties," *Acta Physico-Chimica Sinica*, vol. 31, no. 12, pp. 2332–2340, 2015.

[12] Z.-H. Sheng, L. Shao, J.-J. Chen, W.-J. Bao, F.-B. Wang, and X.-H. Xia, "Catalyst-free synthesis of nitrogen-doped graphene via thermal annealing graphite oxide with melamine and its excellent electrocatalysis," *ACS Nano*, vol. 5, no. 6, pp. 4350–4358, 2011.

[13] E. Vasilaki, I. Georgaki, D. Vernardou, M. Vamvakaki, and N. Katsarakis, "Ag-loaded TiO_2/reduced graphene oxide nanocomposites for enhanced visible-light photocatalytic activity," *Applied Surface Science*, vol. 353, pp. 865–872, 2015.

[14] S. L. Li, Y. B. Wei, L. L. Bai et al., "Preparation and photocatalytic activiyof Co-doped TiO_2/RGO nanocomposites," *Fine Chemicals*, vol. 36, no. 4, pp. 744–750, 2019.

[15] F. Mei, C. Liu, L. Zhang et al., "Microstructural study of binary TiO_2:SiO_2 nanocrystalline thin films," *Journal of Crystal Growth*, vol. 292, no. 1, pp. 87–91, 2006.

[16] H. Ding, N. Zhang, F. Rong, and D.-G. Fu, "Preparation, characterization and bactericidal activity of N-F-codoped TiO_2 film," *Journal of Inorganic Materials*, vol. 26, no. 5, pp. 517–522, 2011.

[17] J. C. Yu, J. Yu, W. Ho et al., "Effects of F-doping on the photocatalytic activity and microstructures of nanocrystalline TiO_2 powders," *Chemistry of Materials*, vol. 14, no. 9, pp. 3808–3816, 2002.

[18] D. Bersani, P. P. Lottici, and X. Z. Ding, "Phonon confinement effects in the Raman scattering by TiO_2 nanocrystals," *Applied Physics Letters*, vol. 72, no. 1, pp. 73–75, 1998.

[19] Q. Zhang, L. Gao, and H. Xie, "Analysis of the structure of titanium tetrachloride derived precipitates," *Materials Science and Engineering A*, vol. 343, no. 1-2, pp. 22–27, 2003.

[20] M. A. Fox and M. T. Dulay, "Heterogeneous photocatalysis," *Chemical Reviews*, vol. 93, no. 1, pp. 341–357, 1993.

[21] L. Jiang, K. Li, L. Yan et al., "Preparation of Ag(Au)/Graphene-TiO_2 composite photocatalysts and their catalytic performance under simulated sunlight irradiation," *Chinese Journal of Catalysis*, vol. 33, no. 12, pp. 1974–1981, 2012.

[22] J. Yu, M. Fan, B. Li et al., "Preparation and photocatalytic activity of mixed phase TiO_2-graphene composites," *Acta Physico-Chimica Sinica*, vol. 31, no. 3, pp. 519–526, 2015.

[23] H. Yun, J. Zhang, M. Minagawa et al., "The origin of the decline in the photocatalytic activity of TiO_2 in the decomposition of NO: TPD spectra of the adsorbed NO species," *Research on Chemical Intermediates*, vol. 29, no. 2, pp. 125–135, 2003.

[24] D. Wang, X. Li, J. Chen, and X. Tao, "Enhanced photoelectrocatalytic activity of reduced graphene oxide/TiO_2 composite films for dye degradation," *Chemical Engineering Journal*, vol. 198-199, pp. 547–554, 2012.

[25] F. Chen, J. Zhao, and H. Hidaka, "Adsorption factor and photocatalytic degradation of dye-constituent aromatics on the surface of TiO_2 in the presence of phosphate anions," *Research on Chemical Intermediates*, vol. 29, no. 7–9, pp. 733–748, 2003.

[26] R. W. Matthews and S. R. Mcevoy, "Photocatalytic degradation of phenol in the presence of near-UV illuminated titanium dioxide," *Journal of Photochemistry & Photobiology A Chemistry*, vol. 64, no. 2, pp. 231–246, 1992.

[27] F. S. Hu, "Adsorption and photocatalytic kinetics of azo dyes," *Acta Physico-Chimica Sinica*, vol. 19, no. 1, pp. 25–29, 2003.

[28] L. Zhou, Y. Shao, J. Liu et al., "Preparation and characterization of magnetic porous carbon microspheres for removal of methylene blue by a heterogeneous Fenton reaction," *Acs Applied Materials & Interfaces*, vol. 6, no. 10, pp. 7275–7285, 2014.

[29] Q. Wang and H. H. Zhang, "Hydrothermal synthesis of N doped TiO_2/graphene composite with visible light photocatalytic activity," *New Chemical Materials*, vol. 45, no. 4, pp. 187–189, 2017.